"Virtual Reality": Electromagnetic Decays and New Hadrons

L.G. Landsberg
Institute for High Energy Physics, Protvino, Russia

In this talk the Coulomb production reactions at high energy are discussed as well as the study of electromagnetic properties of hadrons (mesons and hyperons) in these processes. The results of previous investigations are summed together with some recent data of SELEX(Fermilab) and SPHINX(IHEP) experiments.

1. Introduction

Investigation of electromagnetic hadron decays plays an important role in elementary-particle physics. These processes, governed by the interaction of real and vitual photons with the electric charges of quark fields, make it possible to obtain unique information on the character of various quark configurations in hadrons, the mechanism of mixing, the electromagnetic structure of strongly interacting particles, and on some phenomenological features of such particles (magnetic moments, formfactors, polarizability, etc.). Recent years have seen a significant progress in this field.

Radiative hadron decays of the type $a \to h + \gamma$ can be studied by both direct and indirect methods. In the former case, particle a is produced in a reaction and its decay $a \to h + \gamma$ is detected directly in the experimental setup. Among indirect methods one should mention the process of interaction of primary particle h with a virtual photon in the Coulomb field of the nucleus

$$h + (Z, A) \to a + (Z, A) \tag{1}$$

(see diagram in Fig.1). As we will show later, at a very high energy E_h Coulomb reaction (1) is characterized by small values of the squared 4-momentum transfer q^2 which is identical with the squared 4-momentum q^2 of the virtual photon propagator in Fig.1. Thus, at $q^2 \simeq 0$ the virtual photons are quasi-real. In this approximation the cross section for this Coulomb production process is proportional to the radiative width $\Gamma(a \to h + \gamma)$.

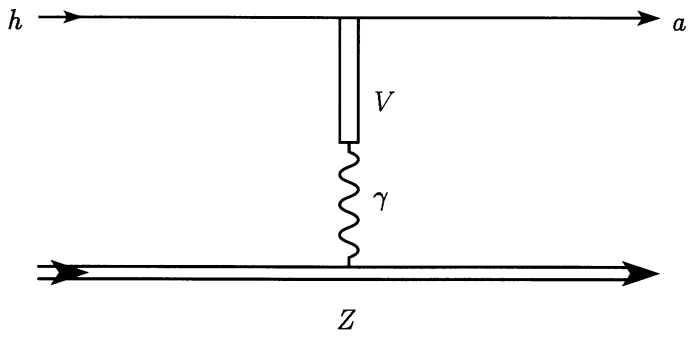

Figure 1: Diagram for the Coulomb process $h + (Z, A) \to a + (Z, A)$. The cross section for this reaction is proportional to the radiative width $\Gamma(a \to h\gamma)$. Symbol V denotes the vector mesons in the $ha\gamma$ vertex in the vector-dominance model.

The main aim of my talk is to discuss these electromagnetic Coulomb processes and their application to the study of radiative decays of hadrons and to the search for some exotic

states. Actually, the type (1) reactions involving collisions with virtual (quasireal) photons ("virtual reality") are photoproduction reactions on primary hadrons h. With pion, kaon, or hyperon beams we have unique possibility to study photoproduction on unstable "targets" (π, K, Y). The Coulomb production mechanism was considered for the first time independently by H.Primakoff [1] and by I. Pomeranchuk and I. Schmushkevich [2]. It is often designated as the Primakoff production or Primakoff reaction.

2. Direct Methods of Studying the Radiative Decays of Hadrons

In this type of experiments the particles under study (a) are produced either in hadron reactions or in electromagnetic interactions (photoproduction; resonance production in e^+e^- collisions). As a rule, to select rare electromagnetic decays

$$a \to h + \gamma, \tag{2}$$

$$a \to b_1 + b_2 + \gamma, \tag{3}$$

it is necessary to detect all the decay products — charge particles as well as photons — to measure their momenta and energy and to reconstruct the effective mass of decay particles ($M(h\gamma)$; $M(b_1b_2\gamma)$).

In the directly detected $a \to h+\gamma$ decays or more intricate electromagnetic processes, we must suppress a background from the decay $\pi^0 \to \gamma\gamma$ with one photon being lost. A similar situation prevails, for example, in searches for the decay $\omega \to \pi^+\pi^-\gamma$ against the background from the main decay mode $\omega \to \pi^+\pi^-\pi^0$, $\pi^0 \to \gamma(\gamma)$ [hereafter, (γ) stands for the lost photon]. Reliable separation of rare radiative decays involving single photons requires a complete detection of all secondaries (both charged and neutral ones), measurement of their momenta, and reconstruction of effective masses with the highest possible resolution. The background from the lost photons can be minimized by equipping the setup with a veto system consisting of counters with a low threshold for photon detection and having the maximum possible coverage. This system also includes a hodoscopic γ spectrometer detecting photons from radiative decays in the operating acceptance of the setup. A strong kinematical constraint on the processes in question can also play an important role. The point is that the background from the events with a lost photon does not yield a narrow peak at the mass of a particle under study and can therefore be considerably reduced owing to kinematical constraints. The above is illustrated by searches for the radiative dacay $\omega \to \pi^+\pi^-\gamma$ in the experiments with the Lepton-F [3] and ASTERIX [4] setups. The background from the lost photons was substantially suppressed by appropriately chosen conditions and using a veto system in the former case and by imposing more stringent kinematical constraints in the latter case. As a result, the two experiments yield approximately the same upper limit on the probability of the above radiative dacay: $BR(\omega \to \pi^+\pi^-\gamma) < 4 \times 10^{-3}$ (at a 95% C.L.) This demonstrates that radiative decays can be sought directly even if their probabilities are less than 1% of the probabilities of the most dangerous background processes. At the same time, the decay $\omega \to \pi^0\pi^0\gamma$, for which the background conditions proved to be much more favourable (the process $\omega \to 3\pi^0$, which could mimic the decay $\omega \to \pi^0\pi^0\gamma$ because of the lost photon, is forbidden by P and C conservation in strong and electromagnetic interactions), was recorded at a significantly lower level of $BR(\omega \to \pi^0\pi^0\gamma) = (7.2 \pm 2.6) \times 10^{-5}$ [5]. The same is true for several other electromagnetic decays with a relatively small background. The results of several experiments for the direct study of rare radiative decays of mesons are presented in Table 1 and in [3-10]. An overview of various methods for detecting electromagnetic decays is given, for example, in review papers [11-14].

Table 1: Direct study of rare radiative decays of light mesons.

Experiment	Process under study	Result	Note
LEPTON-F (IHEP) [3] $\omega \to \pi^+\pi^-\gamma$	$\pi^- + p \to \omega + n$ $(P_{\pi^-} = 38$ GeV) $\hookrightarrow \pi^+\pi^-\gamma$	$BR[\omega \to \pi^+\pi^-\gamma] < 4 \cdot 10^{-3}$ (95% C.L.)	Complicated background conditions due to the main decay channel with one lost photon: $\omega \to \pi^+\pi^-\pi^0 \to$ $\to \pi^+\pi^-\gamma(\gamma)$
ASTERIX (CERN) [4] $\omega \to \pi^+\pi^-\gamma$	$\bar{p}p \to \pi^+\pi^-\omega$ (annihilation $\hookrightarrow \pi^+\pi^-\gamma$ at rest)	$BR[\omega \to \pi^+\pi^-\gamma] < 4 \cdot 10^{-3}$ (95% C.L.)	
GAMS-2000 (IHEP-CERN)[5] $\omega \to \pi^0\pi^0\gamma$	$\pi^- + p \to [\pi^0\pi^0\gamma] + n$ $(P_{\pi^-} = 38$ GeV) $\to \omega + n$ $\hookrightarrow \pi^0\pi^0\gamma$ 40 ± 12 events of the decay $\omega \to \pi^0\pi^0\gamma$ have been observed	$BR[\omega \to \pi^0\pi^0\gamma] =$ $=(7.2 \pm 2.6) \cdot 10^{-5}$	Favourable background conditions (no decays $\omega \nrightarrow 3\pi^0 \to$ $\to \pi^0\pi^0\gamma(\gamma)$)
GAMS-2000 (IHEP-CERN)[6] $\eta \to \pi^0\gamma\gamma$	$\pi^- + p \to \eta + n$ $(P_{\pi^-} = 38$ GeV) $\hookrightarrow \pi^0\gamma\gamma$ Around 70 events $\eta \to \pi^0\gamma\gamma$ have been observed	$BR[\eta \to \pi^0\gamma\gamma] =$ $=(9.5 \pm 3.2) \cdot 10^{-4}$	Favourable background conditions (main background is with 2 lost γ: $\eta \to 3\pi^0 \to \pi^0\gamma(\gamma)\gamma(\gamma)$)
LEPTON-F (IHEP) [7,8] $D/f_1(1285) \to \phi\gamma$	$\pi^- + p \to K^+K^-\gamma + n$ $(P_{\pi^-} = 32,5$ GeV) $\to \phi\gamma + n$ $\hookrightarrow K^+K^-$ 19 ± 5 events of the decay $D/f_1(1285) \to \phi\gamma$ have been detected	$BR[f_1(1285) \to \phi\gamma] =$ $=(0.9 \pm 0.2 \pm 0.4) \cdot 10^{-3}$	Favourable background conditions (no decays $D/f_1 \nrightarrow \phi\pi^0 \to \varphi\gamma(\gamma)$)
LEPTON-G (IHEP) [9-11] $\eta \to \mu^+\mu^-\gamma$ $\eta' \to \mu^+\mu^-\gamma$	$\pi^- + p \to [\mu^+\mu^-\gamma] + n$ $(P_{\pi^-} = 32,5$ GeV) $\to \eta; \eta' + n$ $\hookrightarrow \mu^+\mu^-\gamma$ ~ 600 events of the decay $\eta \to \mu^+\mu^-\gamma$ and 33 ± 7 events of the decay $\eta' \to \mu^+\mu^-\gamma$ have been observed	$BR[\eta \to \mu^+\mu^-\gamma] = (3.4 \pm 0.4) \cdot 10^{-4}$ $BR[\eta' \to \mu^+\mu^-\gamma] = (8.9 \pm 2.4) \cdot 10^{-5}$ Measurements of electromagnetic formfactors of η and η' mesons	Favourable background conditions (no decays $\eta, \eta' \to \mu^+\mu^-\pi^0 \to$ $\to \mu^+\mu^-\gamma(\gamma)$)

3. Coulomb production of hadrons and the study of their radiative decays

To determine the radiative widths of some excited hadrons for which direct measurements involve considerable difficulties or are impossible, it was proposed long ago to use coherent electromagnetic production of particles in the Coulomb field of heavy nuclei ([1,2]), see also [15-18]). The diagram for the Coulomb production of particles in reaction (1) is shown in Fig. 1. In the small-width approximation as applied to the resonance state a in (1), the cross section for electromagnetic production has the from

$$\left[\frac{d\sigma[h+(Z,A)\to a+(Z,A)]}{dq^2}\right]_{\rm Coul} = \\ = |T_{\rm Coul}|^2 = 8\pi\alpha Z^2\cdot\frac{2J_a+1}{2J_h+1}\cdot\Gamma(a\to h\gamma) \\ \times\left[\frac{(q^2-q^2_{\rm min})}{q^4}\right]\cdot\left(\frac{M_a}{(M_a^2-M_h^2)^3}\right)^3\cdot|F_Z(q^2)|^2, \tag{4}$$

where Z is the charge of the nucleus; α is the fine-structure constant; $\Gamma(a\to h\gamma)$ is the radiative decay width of particle a; J_a and J_h are the spins of particles a and h, respectively; M_a and M_h are their masses; $F_Z(q^2)$ is the nuclear electromagnetic form factor; $q^2_{\rm min}=(M_a^2-M_h^2)^2/4E_h^2$ is the minimum 4-momentum transfer squared; and E_h is the energy of the primary particle h. If photons appear as primary particles, an additional factor of two must be included in the expression for the differential cross section.

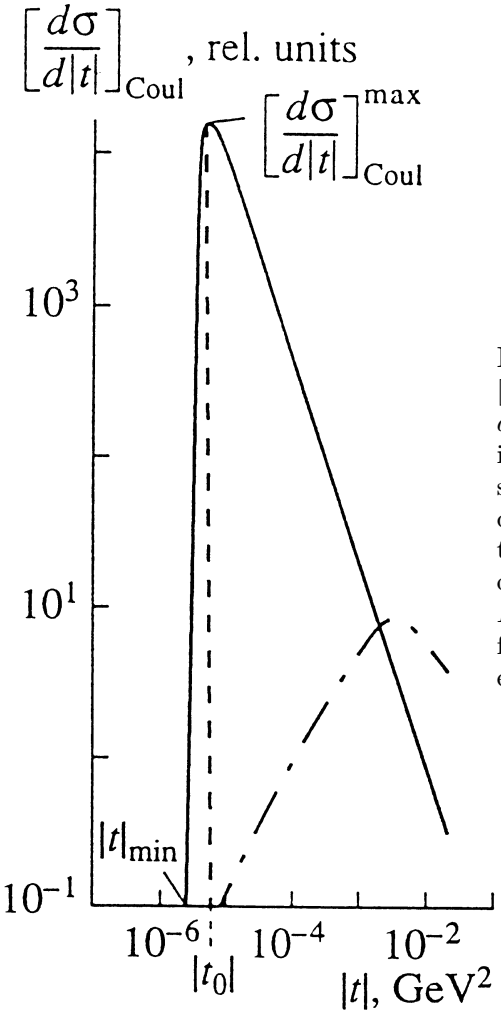

Figure 2: Schematic behavior of the differential cross sections $[d\sigma/dt]_{\rm Coul}$ for the Coulomb-production process $h+(Z,A)\to a+(Z,A)$ (see the diagram in Fig.1). In this figure, $|t|=q^2$ is the squared momentum transfer, and $q_0^2=|t_0|=2|t_{\rm min}|$ the squared momentum transfer that corresponds to the maximum differential cross section $[d\sigma/dt]^{\rm max}_{\rm Coul.}$ (the maximum cross section grows with energy in proportion to E_h^2, while the position of the peak shifts toward lower $|t_0|$ values according to the E_h^{-2} law). The dash-dotted curve represents the background from the coherent process due to strong interaction (with ω exchange).

Figure 2 illustrates schematically the behavior of the differential cross section for the Coulomb particle production. The Coulomb cross section increases fast with decreasing q^2. From expression (4), it can easily be found that the cross section $[d\sigma/dq^2]_{\rm Coul}$ attains a maximum at $q_0^2 = 2q_{\rm min}^2$ and that $[d\sigma/dq^2]^{\rm max}_{\rm Coul} \propto q_{\rm min}^{-2} \propto E_h^2$. As the primary momentum increases, the cross-section value at the maximum increases in proportion to E_h^2, whereas the position of this maximum shifts toward lower values of q^2. The total cross section for the Coulomb process increases as $\ln E_h$. Concurrently, the differential cross section for a coherent process that is governed by a strong interaction exhibits a much broader distribution in q^2, and the region of small q^2 is dominated by the Coulomb contribution. The total Coulomb production cross section has the form

$$\begin{aligned}\sigma[h+(Z,A)\to a+(Z,A)]_{\rm Coul} = \\ = \frac{2J_a+1}{2J_h+1}\cdot 8\pi\alpha Z^2\Gamma(a\to h\gamma)\left(\frac{M_a}{M_a^2-M_h^2}\right)^3\times \\ \times\int_{q_{\rm min}^2}^{q_{\rm max}^2}\frac{(q^2-q_{\rm min}^2)}{q^4}|F_Z(q^2)|^2 d(q^2) = \sigma_0\cdot\Gamma(a\to h\gamma).\end{aligned} \tag{5}$$

The quantity $q_{\rm max}^2$ bounds the integration domain dominated by Coulomb processes. Certainly, a more precise expression for σ_0 can be obfained and used in the data analysis, in which $a\to h\gamma$ decay is expressed more carefully, in a relativistic Breit-Wigner resonance form.

The coherent production of hadrons by a primary particle h on nuclei (Z,A) is a rather complicated process affected by both electromagnetic and strong interactions. The contribution of strong interactions leads to a broader distribution in momentum transfer squared q^2. The differential cross section for coherent particle production on nuclei can be represented as

$$\left[d\sigma/dq^2\right]_{\rm Coherent} = \left|T_{\rm Coul.} + e^{i\varphi}T_{\rm strong}\right|^2, \tag{6}$$

where $T_{\rm Coul.}$ is the amplitude of Coulomb production, $T_{\rm strong}$ is the amplitude of a coherent process that is governed by a strong interaction, and φ is the relative phase of the two amplitudes. For the understanding of a possibility to separate these coherent processes it is instructive to formulate their main characteristics which is done in Table 2.

Table 2: The main features of the Coulomb production processes and the coherent background reactions governed by strong interactions $(h+(Z,A)\to a+(Z,A))$.

Coulomb production processes	Coherent strong interaction reactions	
	ω exchange	Pomeron exchange (diffraction)
a) $\sigma_{\rm Coulomb}\propto lnE_h$. b) $[d\sigma/dq^2]_{\rm Coulomb}$ is in the region of very small q^2 (maximum of cross section is at $q_0^2 = 2q_{\rm min}^2 =$ $= 2[\frac{M_a^2-M_h^2}{2E_h}]^2$. c) The width of $[\frac{d\sigma}{dq^2}]_{\rm Coulomb}$ distribution is $\Delta\sim 6q_{\rm min}^2$. d) $\sigma_{\rm Coulomb}\propto Z^2$. e) In the Gottfrid-Jackson system the t-channel helicity is $\lambda = \pm 1$, which corresponds to quasi-real virtual photon.	a) $\sigma_{\rm strong\ coh.}\sim E_h^{-1}$, e.g. this process died out at the high energies. b) $[d\sigma/dq^2]_{\rm strong\ coh.}$ depends on quantum numbers of particles h and a; in some cases this cross section is reduced in the region of small q^2 as $[\frac{d\sigma}{dq^2}]_{\rm strong\ coh.}\propto(q^2-q_{\rm min}^2)$. c) $\sigma_{\rm strong\ coh.}\propto A^{2/3}$. As a rule this background is small in the region $q^2\le 0.003-0.01$ GeV^2.	a) $\sigma_{\rm strong}$ is practically energy independent (Pomeron exchange). b) $[\frac{d\sigma}{dq^2}]_{\rm strong\ \ coh.}\propto$ $exp[-(q^2-q_{\rm min}^2)b]$ with $b\simeq 10\cdot A^{2/3}$ GeV^{-2}. c) $\sigma_{\rm strong\ \ coh.}\propto A^{2/3}$. d) t-channel helicity $\lambda = 0$. Diffractive coherent processes play a main role if they are allowed by quantum numbers: 1) h and a have the same flavours; 2) $h(J^P)\to$ $\to a[J^P;(J+1)^{-P};(J+2)^P]$ — Gribov-Morrison selection rule.

It can be seen from Table 2 that in accordance with quantum numbers of the produced hadrons in (1) two possible scenarios for the strong coherent background can take place:

A. Coherent diffractive background is forbidden by selection rules for (1) and the leading coherent background is determine usually by ω reggeon exchange in t channel of the reaction. This amplitude dies at a very high energy. In several cases this background is also reduced in the region of small q^2 (as $\propto q^2 - q^2_{\min}$). The absence of diffractive coherent background significantly simplifies the separation of the Coulomb process.

B. Coherent diffractive background plays a leading role in reaction (1). In this case the separation of the Coulomb process is much more difficult and might be performed only in the region of very small $q^2 (< 10^{-3}$ Gev$^2)$ and with a very large statistics.

Let us complete the discussion of the Coulomb production reactions making several conclusions:

1. The Coulomb production reactions open a new possibility to study rare radiative decays $a \to h + \gamma$ if these processes cannot be detected directly due to the background from the decay $a \to h + \pi^0$; $\pi^0 \to \gamma + (\gamma)$ with lost photons or if the decay width is too small for a direct measurement (the later case takes place, for example, for $\Sigma^0 \to \Lambda + \gamma$ decays).

2. The Coulomb production processes open a unique possibily to study the photoproduction reactions on unstable "targets" (like pions, kaons, hyperons), which can be very important for the search for exotic hadrons, for studying some electromagnetic properties of unstable hadrons (their polarizability, for example) and other phenomena.

3. To accomplish this study it is necessary to separate the Coulomb production processes and to make the absolute measurements of their cross sections. All these require very precise and sophisticated experiments in the high energy region. This is the reason for a relatively small amount of the Coulomb production experiments which have been carried out in a 50 year period of time since the first theoretical work of H.Primakoff [1]. The main experimental results in this field at the high energies [19–31] are summarized in Table 3.

4. Study of the Coulomb production processes in the SELEX experiment at $E_h =$ 600 GeV

In 1998 the first prelimimary results of studying several Coulomb production reactions in the SELEX experiment at the Tevatron of Fermilab were obtained and are presented here in short (for more details see [32,33]).

The SELEX setup [34,35], that is used in these measurements includes the three-stage magnetic spectrometer with proportional and drift chumbers, vertex mictrostrip detector, trigger hodoscops, some additional microstrip detectors, RICH and TRD detectors for particle identification, three photon lead glass multichannel spectrometers, neutron calorimeter. The main measurements in the SELEX (E781) experiment were performed with a negative-charged beam of 600 GeV momentum and with practically equal amount of π^--mesons and Σ^--hyperons (they were identified with the beam TRD detector). The wide research program is performed by SELEX(E781) international collaboration (with the participation of scientists from Brasil, China, Germany, Israel, Italy, Mexico, Russia, United Kingdom, USA). The main part of this program involves the study of charmed and strange-charmed baryons, the search for exotic states, the investigation of electromagnetic properties of hadrons and the Coulomb production processes, some other researches. A short summary of the preliminary Coulomb production results in the SELEX experiment is presented below.

Table 3: Results of the Primakoff production processes study.

Experiment	Process under study	Results	Ref.
E272(Fermilab)	$\pi^- + (A,Z) \to \rho(770)^- + (A,Z)$ $(P_{\pi^-} = 156; 260\text{GeV})$ $\hookrightarrow \pi^+\pi^0$	$\Gamma[\rho(770)^- \to \pi^- + \gamma] = 71 \pm 7$ keV	[20]
	$\pi^+ + (A,Z) \to \rho(770)^+ + (A,Z)$ $(P_{\pi^+} = 202\text{GeV})$ $\hookrightarrow \pi^+\pi^0$	$\Gamma[\rho(770)^+ \to \pi^+ + \gamma] = 59.8 \pm 4.0$ keV	[19]
	$\to a_2(1320)^+ + (A,Z)$ $\hookrightarrow \eta\pi^+; K_s^0 K^+$	$\Gamma[a_2(1320)^+ \to \pi^+ + \gamma] = 295 \pm 60$ keV	[21]
	$\to a_1(1260)^+ + (A,Z)$ $\hookrightarrow 3\pi$	$\Gamma[a_1(1266)^+ \to \pi^+ + \gamma] = 640 \pm 246$ keV	[22]
	$\to b_1(1235)^+ + (A,Z)$ $\hookrightarrow \omega\pi^+$	$\Gamma[b_1(1235)^+ \to \pi^+ + \gamma] = 236 \pm 60$ keV	[23]
	$K^- + (A,Z) \to K^*(890)^- + (A,Z)$ $(P_{K^-} = 156\text{GeV})$ $\hookrightarrow K_s^0\pi^-$	$\Gamma[K^{*0}(890)^- \to \pi^- + \gamma] = 62 \pm 12$ keV	[24]
Fermilab	$K_L^0 + (A,Z) \to K^*(896)^0 + (A,Z)$ $(P_{K^0} = 60 - 200\text{GeV})$ $\hookrightarrow K_s^0\pi^0$	$\Gamma[K^{*0}(896)^0 \to K^0 + \gamma] = 116.5 \pm 9.9$ keV	[25]
	$\to K^*(1430)^0 + (A,Z)$ $\hookrightarrow K_s^0\pi^0$	$\Gamma[K^*(1420)^0 \to K^0 + \gamma] < 84$ keV (90% C.L.)	[26]
CERN	$\pi^- + (A,Z) \to \rho(770)^- + (A,Z)$ $(P_{\pi^-} = 200\text{GeV})$ $\hookrightarrow \pi^-\pi^0$	$\Gamma[\rho(770)^- \to \pi^- + \gamma] = 81 \pm 4 \pm 4$ keV	[27]
SIGMA(IHEP)	$\pi^- + (A,Z) \to \pi^-\gamma + (A,Z)$ $(P_{\pi^-} = 40\text{GeV})$ Compton $\gamma\pi$-scattering; measurements of magnetic (β_π) and electric (α_π) polarizability of pion	$\beta_\pi = (-7.1 \pm 2.8 \pm 1.8) \cdot 10^{-43}$ cm^3 $\alpha_\pi + \beta_\pi = (1.4 \pm 3.1 \pm 2.5) \cdot 10^{-43}$ cm^3	[28]
	$\pi^- + (A,Z) \to \pi^-\pi^0 + (A,Z)$	Study of chiral anomaly $F(\gamma \to 3\pi) = 12.9 \pm$ $\pm 0.9 \pm 0.5$ GeV^{-3}	[29]
CERN	$\Lambda + (A,Z) \to \Sigma^0 + (A,Z)$ $\langle P_\Lambda \rangle = 15$ GeV	$\Gamma[\Sigma^0 \to \Lambda + \gamma] = 7.6^{+2.0}_{-1.3}$ KeV	[30]
Fermilab	$\Lambda + (A,Z) \to \Sigma^0 + (A,Z)$ $\langle P_\Lambda \rangle = 200$ GeV	$\Gamma[\Sigma^0 \to \Lambda + \gamma] = 8.6 \pm 0.6 \pm 0.8$ KeV	[31]

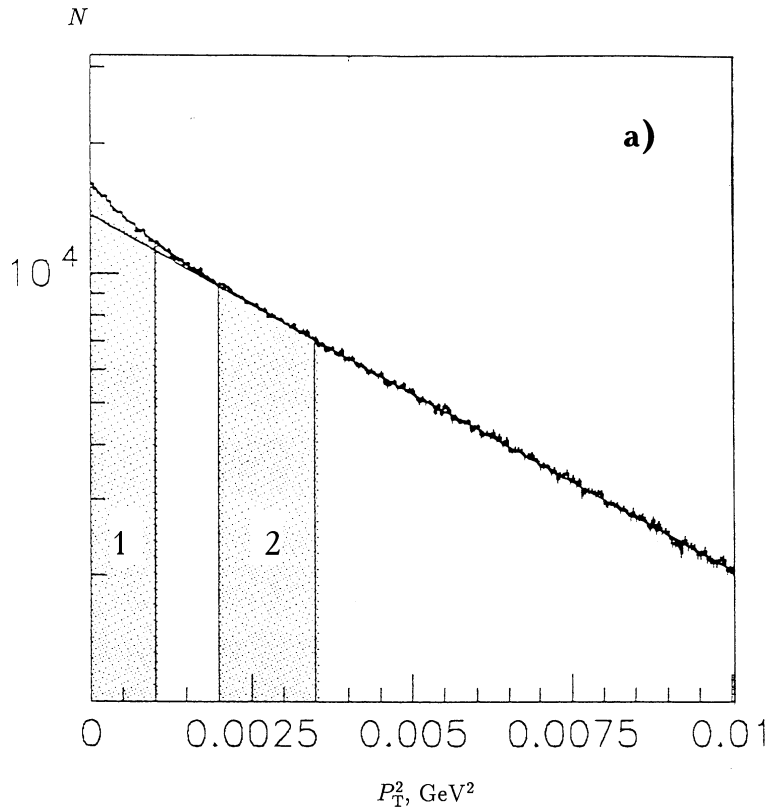
N
a)
10 4
1
2
0
0.0025
0.005
0.0075
0.01
P_T^2, GeV²

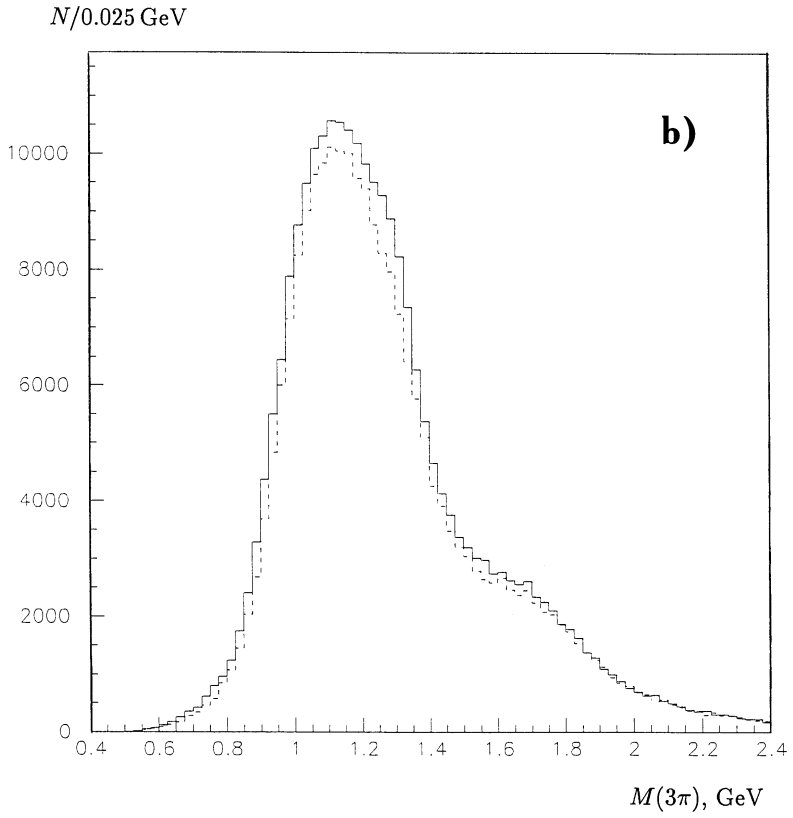
N/0.025 GeV
b)
10000
8000
6000
4000
2000
0
0.4
0.6
0.8
1
1.2
1.4
1.6
1.8
2
2.2
2.4
M(3π), GeV

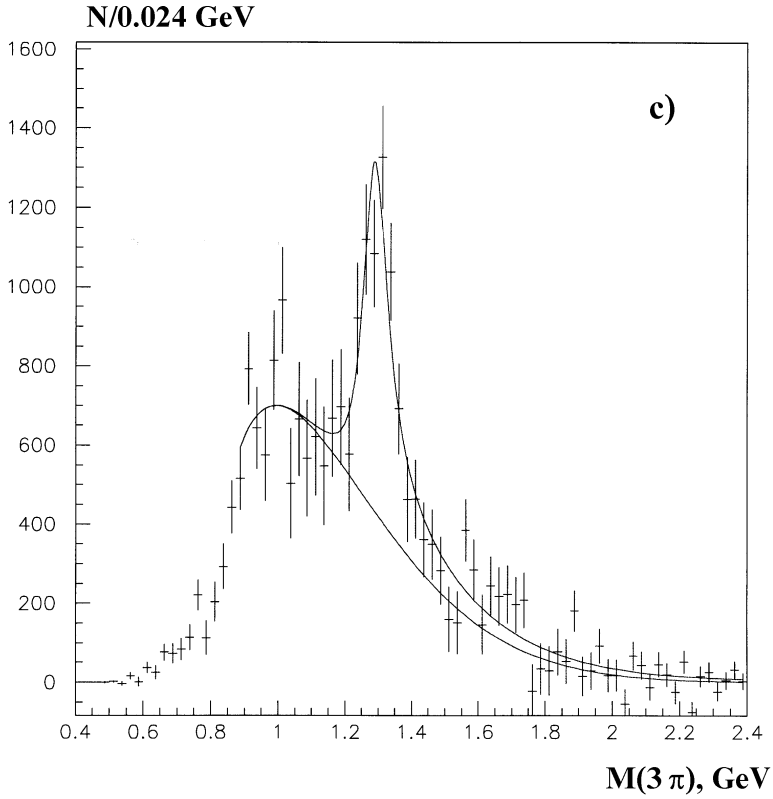

Figure 3: The data for the coherent reaction $\pi^- + Cu \to [\pi^-\pi^-\pi^+] + Cu$ at $E_{\pi^-} = 600$ GeV obtained at the SELEX setup. a) dN/dP_T^2 distribution. The dash line shows the slope for coherent diffraction process caused by the Pomeron exchange. Region 1 ($P_T^2 < 0.001$ GeV^2) and region 2 ($0.0015 < P_T^2 < 0.0035$) are used for the Coulomb production separation and for subtraction of the diffractive coherent background. b) Effective mass spectra $M(3\pi)$ for region 1 (solid line) and for region 2 (dashed line). c) Effective mass spectrum $M(3\pi)$ for the Coulomb production process, obtained by subtraction $M(3\pi)_1 - a \cdot M(3\pi)_2$ after a proper normalization (a — the normalization factor which was chosen in such a way that the number of diffractive background events in $N(3\pi)_1$ and $a \cdot N(3\pi)_2$ were identical).

4.1. Study of the reaction $\pi^- + (A, Z) \to [\pi^-\pi^-\pi^+] + (A, Z)$ and measurment of the radiative width for $a_2(1320)$ meson

The coherent reactions

$$\pi^- + (Z, A) \to [\pi^-\pi^-\pi^+] + (A, Z) \tag{7}$$

on carbon, copper and lead nuclei were separated in the analysis of the events with 3 charge particles in the final state in the interactions of identified primary π^--mesons in one of the targets. These events must satisfy the "elastic conditions" — the difference between the beam particle momentum and the sum of momenta of three secondary particles must be less than 17.5 GeV. The statistics of the selected events of (7) is tabulated in Table 4.

The P_T^2 distribution* of the $(3\pi)^-$-system in reaction (7) for the copper target is shown, as an example, in Fig.3a. This dN/dP_T^2 distribution was fitted by the sum of two exponents $dN/dP_T^2 = C_1 exp(-b_1 P_T^2) + C_2 exp(-b_2 P_T^2)$ with the slopes $b_1 = 1577 \pm 88$ GeV^{-2} and $b_2 = 189.4 \pm 0.6$ GeV^{-2}. The second slope b_2 is in a good agreement with the slope for diffractive production coherent process (7) obtained from the data [36] at $E_\pi = 200$ GeV. The slope b_1 corresponds to the Monte Carlo estimations for the Coulomb mechanism (with account for the P_T^2 resolution).

*Here $q^2 \simeq q^2_{\min} + P_T^2 \simeq P_T^2$ at a very high momentum.

Table 4: Study of the coherent reaction $\pi^- + (A,Z) \to (\pi^-\pi^-\pi^+) + (A,Z)$ and the determination of radiative with $\Gamma[a_2(1320)^- \to \pi^- + \gamma]$.

Target	Number of events $\pi^- + (A,Z) \to$ $\to (3\pi)^- + (A,Z)$	Number of $a_2(1320)$ events produced in the Coulomb process	$\Gamma[a_2(1320)^- \to$ $\to \pi^- + \gamma]$ (keV)	Average value $\Gamma[a_2(1320)^- \to \pi^- + \gamma]$ (keV)	$\Gamma[a_2(1320)^- \to \pi^- + \gamma]$ from [21] (keV)	Theoretical predictions for $\Gamma[a_2(1320)^- \to$ $\to \pi^- + \gamma]$ (keV)
Carbon	2760523	1587 ± 480	289 ± 87			348 [37]
Copper	1997972	5170 ± 590	248 ± 27	$225 \pm 25(\text{stat.}) \pm$	295 ± 60	
Lead	549092	2945 ± 400	198 ± 27	$\pm 45(\text{syst.}) = 225 \pm 51$		235[38]

Two P_T^2 regions were defined for dN/dP_T^2 distribution (see Fig.3a). In the first region ($P_T^2 < 0.001$ GeV^2) the Coulomb production process dominating. The second region ($0.0015 < P_T^2 < 0.0035$ GeV^2) was used to estimate the coherent diffractive background. The mass spectra $M(3\pi)$ for these two regions are presented in Fig. 3b. The result of diffractive background subtraction (after a proper normalization) is presented in Fig. 3c. In this subtracted mass spectrum the Coulomb production of $a_2(1320)^-$ meson in the reaction

$$\begin{array}{rcl} \pi^- + Cu & \rightarrow & a_2(1320)^- + Cu \\ & & \hookrightarrow \pi^-\pi^-\pi^+ \end{array} \quad (8)$$

is clearly seen. The same results were also obtained from the measurements with carbon and lead targets. After the absolute normalization of cross sections for the Primakoff reactions $\sigma_{\rm Coulomb}[a_2(1320)^-] = \sigma_0 \cdot \Gamma[a_2(1320)^- \rightarrow \pi^-\gamma]$, the values for radiative width $\Gamma[a_2(1320)^- \rightarrow \pi^-\gamma]$ from all these measurements were obtained (see Table 4). For the absolute normalization the cross sections of diffractive production reactions (7) for $A = Pb$; Cu; C from [36] were used.

The data for the radiative width in the measurements with different targets are consistent with each other, which confirms the Coulomb production of $a_2(1320)$ meson. The average value of radiative width over all the targets is

$$\Gamma[a_2(1320)^- \rightarrow \pi^-\gamma] = 225 \pm 20(\text{stat.}) \pm 45(\text{syst.}) \text{ keV}. \quad (9)$$

The main source for the systematic uncertainty is the absolute normalization procedure. This value of the radiative width is preliminary and might be obtained with a better accuracy in the future. The comparison of value (10) with previous measurement [21] and with theoretical predictions [37, 38] is also presented in Table 4.

4.2. Further Primakoff reaction data from the SELEX experiment

4.2.1. Study of the coherent reactions

$$\begin{array}{rcll} \pi^- + (A,Z) & \rightarrow & [\pi^-\pi^-\pi^+\pi^0] + (A,Z), & (10) \\ & & \hookrightarrow \gamma\gamma & \\ & \rightarrow & [\pi^-\omega] + (A,Z), & (11) \\ & & \hookrightarrow \pi^+\pi^-\pi^0 & \\ & \rightarrow & b_1(1235) + (A,Z), & (12) \\ & & \hookrightarrow \omega\pi^- & \\ & \rightarrow & [\pi^-\eta] + (A,Z), & (13) \\ & & \hookrightarrow \pi^+\pi^-\pi^0 & \\ & \rightarrow & a_2(1235) + (A,Z), & (14) \\ & & \hookrightarrow \pi^-\eta & \end{array}$$

were performed at $E_{\pi^-} = 600$ GeV on the lead, copper and carbon targets in the SELEX experiment. The Coulomb production of $b_1(1235)^- \rightarrow \omega\pi^-$ and $a_2(1320)^- \rightarrow \eta\pi^-$ was observed quite clearly in (12) and (14) under very favourable background conditions (see, for example, Fig.4). The Coherent strong interaction background here is dominated by ω exchange and is small in the region of $P_T^2 < 0.003$ GeV^2. Now the data from these Primakoff reactions are in the course of analysis to obtain the absolute normalization of their cross sections and to determine the radiative widths $\Gamma[b_1(1235)^- \rightarrow \pi^- + \gamma]$ and $\Gamma[a_2(1320)^- \rightarrow \pi^- + \gamma]$.

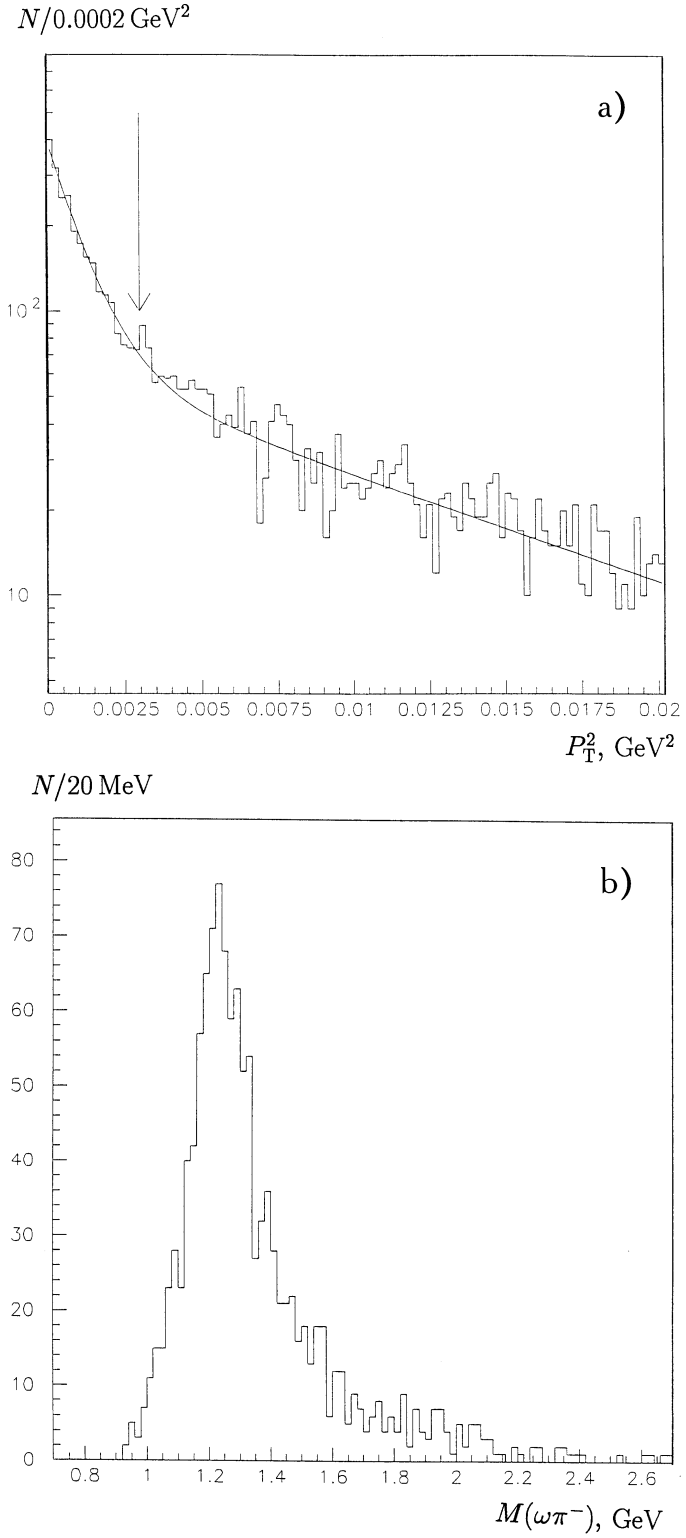

Figure 4: The data for the reaction $\pi^- + (A, Z) \to [\omega\pi^-] + (A, Z)$ at $E_{\pi^-} = 600$ GeV obtained in the experiment at the SELEX setup (summed data for C, Cu and Pb targets). a) dN/dP_T^2 distribution. In this distribution the Coulomb production is dominated in the region of small P_T^2 ($P_T^2 < 0.003$ GeV^2, pointed by an arrow). For this reaction the coherent strong interaction background is small (it is governed by ω exchange). b) Effective mass spectrum $M(\omega\pi^-)$ for the Coulomb production region $P_T^2 < 0.003$ GeV^2. In this spectrum the Coulomb production of $b_1(1235)^- \to \omega\pi^-$ is clearly seen.

4.2.2. Study of the Coulomb production reaction

$$\Sigma^- + Pb \to \Sigma^*(1385)^- + Pb. \tag{15}$$

This Primakoff process is determined by a very small width of SU(3) forbidden radiative decay

$$\Sigma^*(1385)^- \to \Sigma^- + \gamma. \tag{16}$$

Only a short didicated run at the SELEX facility can be used for the study of Primakoff reaction (15). The preliminary value for the upper limit of radiative width for decay (16) is obtained in this measurement

$$\Gamma[\Sigma^*(1385)^- \to \Sigma^- + \gamma] < 7\text{KeV} \quad (95\text{c.l.}) \tag{17}$$

The theoretical expectations for this width are in the region of 1– 10 KeV (see reviews [39,40] and the references herein). For comparison, the expected value of radiative width for the SU(3) allowed decay

$$\Sigma^*(1385)^+ \to \Sigma^+ + \gamma \tag{18}$$

is predicted at a level of 100 keV.

5. Coulomb reactions and the search for exotics

The Coulomb production processes ("Primakoff reactions") can be of great concern not only in the study of radiative hadronic decays, but in the search for new types of hadrons as well. In the last decade the problem of existence of a novel form of hadronic matter — exotic hadrons — has become the leading direction in hadron spectroscopy. A rapid development of this field led to a significant advance in the systematics of "ordinary" hadrons (with the valence quark structure $q\bar{q}$ or qqq) and to the observation of several unusual states which do not fit this simplest systematics. These anomalous states are real candidates for exotic hadrons with a complicated valence internal structure (multiquark formations $qq\bar{q}\bar{q}$, $qqqq\bar{q}$; hybrid states with valence quarks and gluons $q\bar{q}g$, $qqqg$; pure gluonic mesons — glueballs gg, ggg).

The success of experiments aimed at the search for exotic hadrons and first of all for cryptoexotic states with usual quantum numbers but with anomalous dynamical properties ("hidden exotics") is, to a great extent, determined by the appropriate choice of the production processes for which some qualitative considerations can predict more distinct manifestations of exotic states. For example, it was emphasized in a number of studies that gluon-rich diffractive production reactions on nucleons or nuclei (coherent reactions) offer some favourable grounds for exotic hadron production [41–44]. It was also stated that for some cases the electromagnetic mechanisms can be very promising for these aims [45–47].

Let us consider, for example, the exotic hadrons with hidden strangeness — $q\bar{q}s\bar{s}$ mesons or $qqqs\bar{s}$ baryons (here $q = u$- or d-quarks). Due to a significant coupling of photon with $s\bar{s}$ pairs through ϕ meson in the framwork of VDM, electromagnetic interactions can provide a natural way to embed the $s\bar{s}$ pair into an intermediate hadron state and to produce the exotic hadron with hidden strangeness. This possibility is illustrated by Fig.5a for the resonance s-channel reaction

$$\gamma + N \to |qqqs\bar{s}\rangle \to YK \tag{19}$$

or for the Coulomb producton reaction

$$h + (Z, A) \to |qqqs\bar{s}\rangle + (Z, A) \tag{20}$$

(see Fig.5b). As has been shown in Section 3, the Coulomb production mechanism plays the leading role in the region of very small transfer momenta, where it is dominating over the strong interaction process. Thus, the coherent reactions at a very small $P_T^2 (\lesssim 0.01$ GeV$^2)$ can be used in the search for exotic states with hidden strangeness.

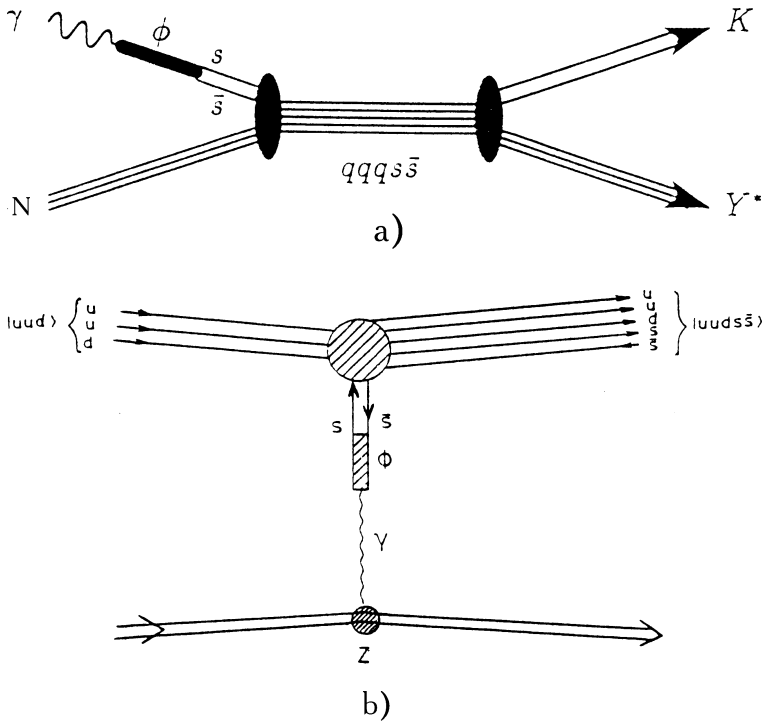

Figure 5: Electromagnetic mechanisms for production of exotic baryons with hidden strangeness: a) formation reaction with s-channel resonance photoproduction; b) Coulomb production reaction $h + (Z, A) \to a + (Z, A)$.

As was stated before, the most interesting Coulomb production processes were those initiated by unstable primary particles (π-mesons, K-mesons, hyperons), because these processes give the only possibility to study the photoproduction reactions on unstable targets. Reaction (20) for protons ($h \equiv p$) is, in principle, the same as photoproduction process (19) which can be studied in a very detailed way on photon beams of electron accelerators. But the existing data for these reactions are rather poor now and insufficient for such systematical studies. One can hope that in the near future reliable data would be obtained in the experiments at strong current electron accelerators CEBAF and ELSA (see, for example, [48]).

On the other hand, there are the data for coherent reactions

$$p + C \to [Y^0 K^+] + C \tag{21}$$

obtained in the experiments of the SPHINX Collaboration which might be connected with the Coulomb production mechanism. We will discuss these data in the next Section.

6. The experiments of the SPHINX Collaboration and the search for exotic baryons with hidden strangeness

Extensive study of the diffractive baryon production and search for cryptoexotic pentaquark baryons with hidden strangeness ($B_\phi = |qqqs\bar{s}\rangle$), are being carried out by the SPHINX Collab-

oration at the IHEP accelerator with a 70 GeV proton beam. This program was described in detail in reviews [44].

The cryptoexotic B_ϕ baryons do not have external exotic quantum numbers and their complicated internal valence structure can be established only indirectly, by examination of their unusual dynamic properties which are quite different from those for ordinary $|qqq\rangle$ baryons. Examples of such anomalous features are listed below (see [44] for more details):

(i) The dominant OZI-allowed decay modes of the baryons B_ϕ are those with strange particles in the final states:

$$R(|qqqs\bar{s}\rangle) = BR[|qqqs\bar{s}\rangle \to YK]/BR[|qqqs\bar{s}\rangle \to p\pi\pi; \Delta\pi] \gtrsim 1. \tag{22}$$

For ordinary $|qqq\rangle$ isobars $R(\Delta; N^*) \sim$ (several %)[49,50].

(ii) The cryptoexotic baryons B_ϕ can possess simultaneously a large mass ($M > 1.8 - 2.0$ GeV) and a narrow decay width ($\Gamma \leq 50 \div 100$ MeV). This is due to a complicated internal color structure of these baryons, which leads to a significant quark rearrangement of color clusters in decay processes, and due to a limited phase space for the OZI-allowed decays $B_\phi \to YK$. At the same time, typical decay widths of the well-established $|qqq\rangle$ isobars with similar masses are no less than 300 MeV [49].

Several diffractive production reactions were studied in the experiment of the SPHINX Collaboration:

$$p + N(A) \quad \to \quad [pK^+K^-] + N(A) \tag{23}$$

$$\to \quad (p\phi) + N(A), \qquad \hookrightarrow K^+K^- \tag{24}$$

$$\to \quad [\Sigma^*(1385)^0 K^+] + N(A), \qquad \hookrightarrow \Lambda\pi^0 \tag{25}$$

$$\to \quad [\Sigma^0 K^+] + N(A), \qquad \hookrightarrow \Lambda\gamma \tag{26}$$

$$\to \quad [p\eta] + N(A) \qquad \hookrightarrow \pi^+\pi^-\pi^0 \tag{27}$$

$$\to \quad [p\eta'] + N(A), \qquad \hookrightarrow \pi^+\pi^-\eta \to \pi^+\pi^- 2\gamma \tag{28}$$

$$\to \quad [p\pi^+\pi^-] + N(A) \tag{29}$$

$$\to \quad [\Delta^{++}\pi^-] + N(A) \tag{30}$$

(here N is nucleon and A is nucleus for coherent reaction).

The SPHINX detector used in these measurements includes a wide-aperture magnetic spectrometer with scintillator hodoscopes, proportional wire chambers, drift chambers, drift tubes and a multichannel γ-spectrometer made of total absorption lead glass detectors. Charged particles of the final state were identified with a differential RICH spectrometer and two multicell gas threshold Čherenkov counters C_1 and C_2. A detailed description of the apparatus can be found in [51,52]. The recent data of the SPHINX experiments gave new important evidence of possible existance of cryptoexotic baryons with hidden strangeness $X(2050)^+ \to \Sigma(1385)^0 K^+$ and $X(2000)^+ \to \Sigma^0 K^+$ (see [50-55]). These data are summarized in Table 5 and in Figs 6–9.

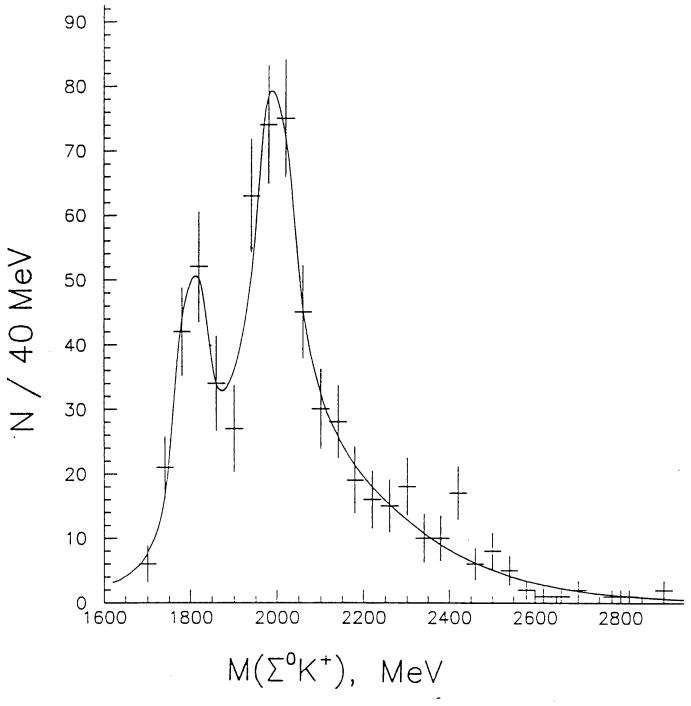

Figure 6: Combined mass spectrum $M(\Sigma^0 K^+)$ for coherent diffraction reaction (26) in the old and new runs at the SPHINX setup ($P_T^2 < 0.1$ GeV^2). The parameters of $X(2000)$ peak in this spectrum are: $M = (1997 \pm 7)$ MeV; $\Gamma = (91 \pm 17)$ MeV.

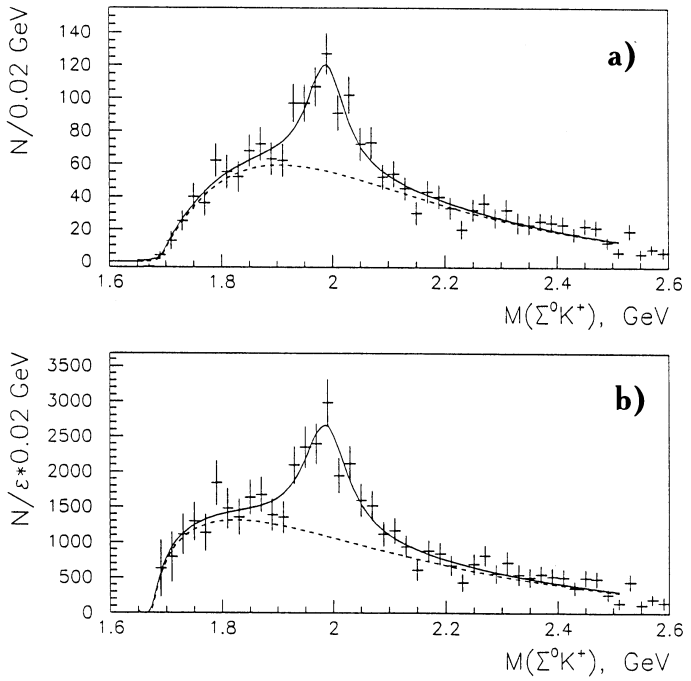

Figure 7: Invariant mass spectra $M(\Sigma^0 K^+)$ in the diffractive reaction $p + N \to [\Sigma^0 K^+] + N$ for all P_T^2: a) measured mass spectrum; b) the same mass spectrum weighted with the efficiency of the setup. Parameters of $X(2000)$ peak are $M = (1986 \pm 6)$ MeV and $\Gamma = (98 \pm 20)$ MeV.

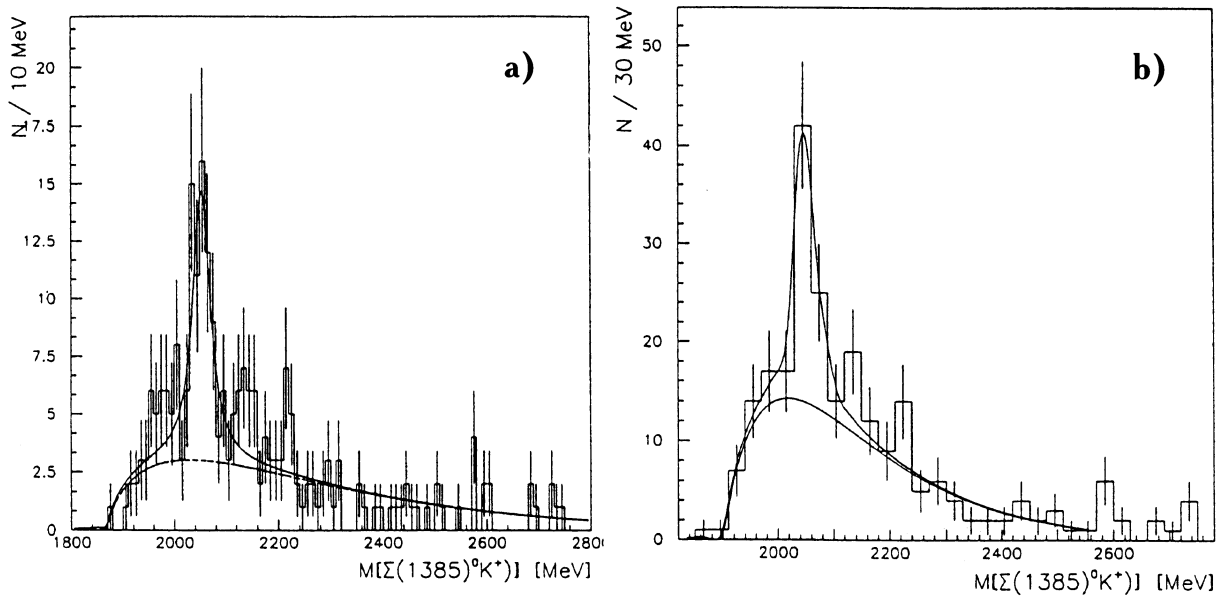

Figure 8: Invariant mass spectra $[\Sigma^*(1385)^0 K^+]$ in coherent reaction (25) at tight transverse-momentum cut $P_T^2 < 0.02$ GeV^2 for various bin widths: a) $\Delta M = 10$ MeV; b) $\Delta M = 30$ MeV. The spectra are fitted to the sum of a smooth polynomial background and $X(2050)$ Breit-Wigner peak. The parameters of $X(2050)$ peak are: a) $M = (2053 \pm 4)$ MeV; $\Gamma = (40 \pm 15)$ MeV; b) $M = (2053 \pm 5)$ MeV; $\Gamma = (35 \pm 16)$ MeV.

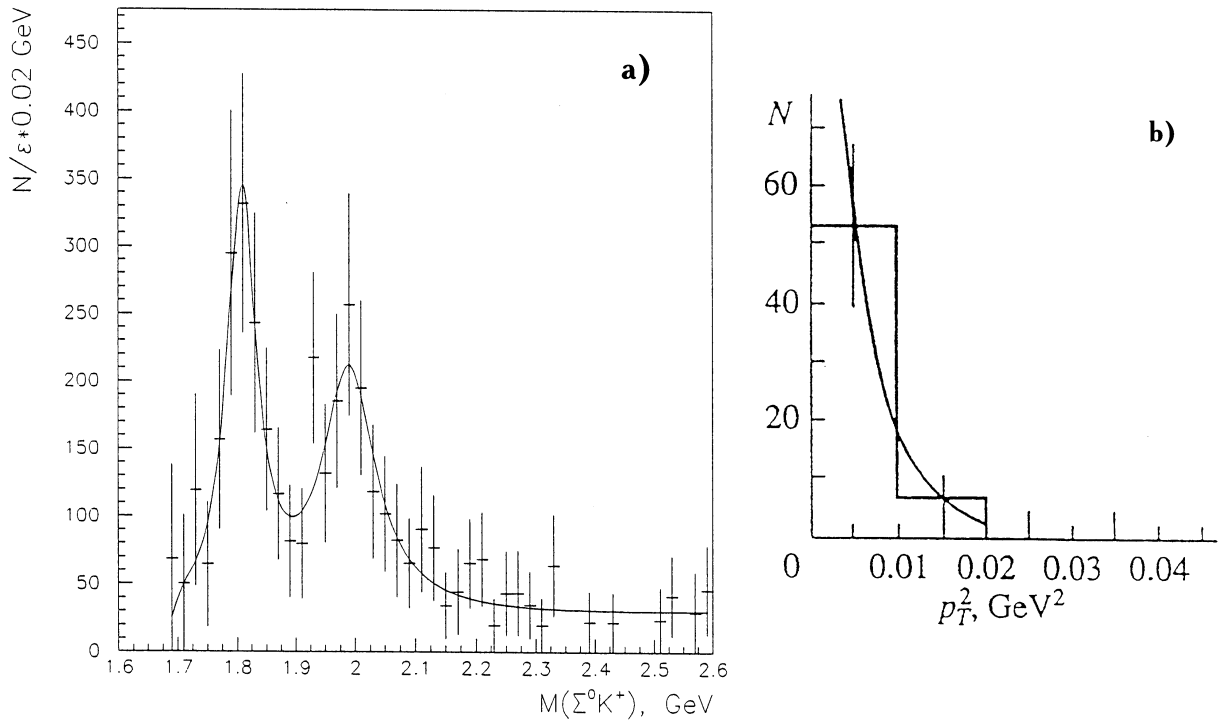

Figure 9: a) Invariant mass spectrum $M(\Sigma^0 K^+)$ in the coherent diffractive production reaction $p + C \to [\Sigma^0 K^+] + C$ in the region of very small transverse momenta ($P_T^2 < 0.01$ GeV^2) weighted with the efficiency of the setup. Parameters of $X(1810)$ peak are $M = (1807 \pm 7)$ MeV and $\Gamma = (62 \pm 19)$ MeV. b) The P_T^2 dependence for the $X(1810)$ structure production in the coherent reaction $p + C \to X(1810) + C$.

Table 5. Results of the search for exotic baryons in diffractive production experiment of the SPHINX Collaboration [50-55].

1.	Coherent diffractive production reaction $p + C \to [\Sigma^0 K^+] + C$ with coherent cut $P_T^2 < 0.1$ GeV^2 was studied in the old and new runs. The combined mass spectrum $M(\Sigma^0 K^+)$ is presented on Fig. 6. This spectrum is dominated by the $X(2000)$ state with parameters $M = (1997 \pm 7)$ MeV, $\Gamma = (91 \pm 17)$ MeV, statistical significance of the peak is 7 s.d. The state $X(2000)$ was also observed in diffractive production reaction $p + N \to [\Sigma^0 K^+] + N$ with all P_T^2 (see Fig. 7).
2.	There is also a near threshold structure $X(1810)$ in the $M(\Sigma^0 K^+)$ mass spectrum, which is produced only in the region of very small $P_T^2 (\lesssim 0.01 \div 0.02$ GeV$^2)$ — see the text.
3.	Coherent diffractive production reaction $p + C \to [\Sigma^*(1385)^0 K^+] + C$ (25) with tight coherent cut $P_T^2 < 0.02$ GeV^2 was studied in the old run. The mass spectra of $M[\Sigma^*(1385)^0 K^+]$ are in Fig. 8. The peak $X(2050)$ was observed in these spectra with an average value of parameters $M = 2052 \pm 6$MeV, $\Gamma = 35^{+22}_{-35}$MeV, (with account for the apparatus mass resolution); statistical C.L. of the peak ≥ 5 s. d. The information for reaction (25) in the new run is now under analysis.
4.	In studying coherent reactions (29) $p + C \to [p\pi^+\pi^-] + C$ and (30) $p + C \to [\Delta(1232)^{++}\pi^-] + C$ under the same kinematical conditions as of processes (26) and (25) the search for other decay channels of the $X(2000)$ and $X(2050)$ baryons was performed. No peaks in 2 GeV mass range were observed in the mass spectra of $p\pi^+\pi^-$ and $\Delta(1232)^{++}\pi^-$ systems produced in reactions (29) and (30). Lower limits for the corresponding decay branching ratios R (see(22)) were obtained from this comparative analysis: $R[X(2000);\ X(2050)] = \Gamma(X \to YK)/\Gamma[X \to \Delta\pi;\ p\pi^+\pi^-] \gtrsim 1 \div 10$ These ratios are by 2 orders of magnitude larger than those for ordinary (qqq) isobars (see [49,50]).
5.	A narrow width of the $X(2000)$ and $X(2050)$ baryon states as well as anomalously large branching ratios for their decay channels with strange particle emission (large values of R) are the reasons for considering these states as serious candidates for cryptoexotic baryons with a hidden strangeness $\|uuds\bar{s}\rangle$.

As was shown in Table 5, in the study of coherent reaction (26) the unusual narrow $X(1810)$ state was observed in the region of very small $P_T^2 (\lesssim 0.01$ GeV$^2)$. The data for the effective mass spectrum $M(\Sigma^0 K^+)$ in reaction (26) for this region is presented on Fig.9. This spectrum demonstrates the sharp peak with parameters

$$X(1810) \to \Sigma^0 K^+ \left\{ \begin{array}{l} M = (1807 \pm 7) \text{ MeV} \\ \Gamma = (62 \pm 19) \text{ MeV} \end{array} \right. \tag{31}$$

The cross section for the coherent $X(1810)$ production is

$$\begin{array}{c} \sigma[p + C \to X(1810)^+ + C]|_{p_T^2 < 0.01 \text{GeV}^2} \cdot BR[X(1810)^+ \to \Sigma^0 K^+] = \\ = 215 \pm 45 \text{ nb/C nucleus} \end{array} \tag{32}$$

The error in this cross section is statistical only. An additional systematic error for this value is ±30% due to uncertainties in the cuts, in the Monte Carlo effeiciency calculations, in the account of the P_T^2 smearing in the region of very small P_T^2 and in the absolute normalization.

To explain the properties of $X(1810)$ state in a very small P_T^2 region, the hypothesis of the electromagnetic production of this state in the Coulomb field of carbon nucleus was proposed earlier [47]. It is possible to estimate the cross section for the Coulomb $X(1810)$ production from (4) and (5):

$$\begin{gathered}\sigma[p+C\to X(1810)^+ + C]|_{P_T^2<0.01\ \mathrm{GeV}^2;\mathrm{Coulomb}} = \\ = (2J_\mathrm{x}+1)\{\Gamma[X(1810)^+\to p+\gamma][\mathrm{MeV}]\}\cdot 2.8\cdot 10^{-30}\mathrm{cm}^2/\mathrm{C\ nucleus} \geq \\ \geq 5.6\cdot 10^{-30}\mathrm{cm}^2\{\Gamma[X(1810)^+\to p+\gamma][\mathrm{MeV}]\}\end{gathered} \tag{33}$$

($J_\mathrm{x}\geq 1/2$ is the spin of $X(1810)$). Let us compare this Coulomb hypothesis prediction with the experimental value

$$\sigma[p+C\to X(1810)^+ + C]|_{P_T^2<0.01\ \mathrm{GeV}^2} \gtrsim 645\mathrm{nb/C\ nucleus}. \tag{34}$$

To obtain (34) we assumed that $X(1810)$ is isodoublet, and then we use (32) with the branching $BR[X^+_{I=1/2}\to\Sigma^0K^+] = \frac{1}{3}BR[X^+_{I=1/2}\to(\Sigma K)^+]\lesssim 1/3$ (here $\simeq$ means that $BR[X^+\to(\Sigma K)^+]\simeq 1$, i.e. this decay is dominating).

If the value of radiative width $\Gamma[X(1810)\to p+\gamma]$ is around 0.1-0.3 MeV and the branching $BR[X(1810)^+\to(\Sigma K)^+]$ is significant, then the experimental data for the cross section of the coherent $X(1810)$ production (34) can be in agreement with the Coulomb mechanism prediction (33). It seems that the assumed value of radiative width is quite reasonable. For example, the radiative width for $\Delta(1232)$ isobar is $\Gamma[\Delta(1232)^+\to p+\gamma]\simeq 0.7$MeV. The value of radiative width depends on the amplitude of this process A and kinematical factor: $\Gamma = |A|^2\cdot(P_\gamma)^{2l+1}$ (P_γ is the momentum of photon in the rest frame of the decay baryon and l is the orbital momentum). For the $X(1810)\to p+\gamma$ decay the kinematical factor may be by an order of magnitude larger than for $\Delta(1232)^+\to p+\gamma$ because of the large mass of $X(1810)$ baryon. Certainly, the predictions for amplitude A are quite speculative. But if, for example, $X(1810)$ is the state with hidden strangeness $|qqqs\bar{s}\rangle$, then the amlplitude A might be not very small due to a possible VDM decay mechanism $(qqqs\bar{s})\to(qqq)+\phi_\mathrm{virt}\to(qqq)+\gamma$. Thus, the experimental study doesn't seem to be in contradiction with the Coulomb production hypothesis.

It is possible for the candidate state $X(2050)\to\Sigma^*(1385)^0K^+$ that was observed in coherent reaction (25) in the region of very small transverse momenta ($P_T^2<0.02$ GeV^2) to be also produced not by the diffractive, but electromagnetic Coulomb production mechanism [47].

The feasibility to separate the Coulomb production processes in the coherent proton reactions at $E_p = 70$ GeV on the carbon target in the measurement with the SPHINX setup has been recently demonstrated in the observation of the Coulomb production of $\Delta(1232)^+$ isobar with $I = 3/2$ in the reaction

$$p+C\to\Delta(1232)^+ + C \tag{35}$$

(see [47] and Fig.10).

7. Conclusion

The recent results of the Coulomb production reactions study presented in this talk allow one to obtain the important information on the electromagnetic properties of hadrons and to search for new hadronic structures. We continue the analysis of the data obtained in the SELEX experiment and we hope to improve the precision of these measurements and the number of

Primakoff reactions under study. The SPHINX experiment is in the run now and in the near future we hope to advance in statistics by an order of magnitude and to obtain new information on exotic baryons and other states.

It is a pleasure for me to express gratitude to my colleagues from the SELEX and SPHINX Collaborations for a tight cooperation in obtaining the main results presented here.

The work is partially supported by RFBR (grant 96-02-16759a).

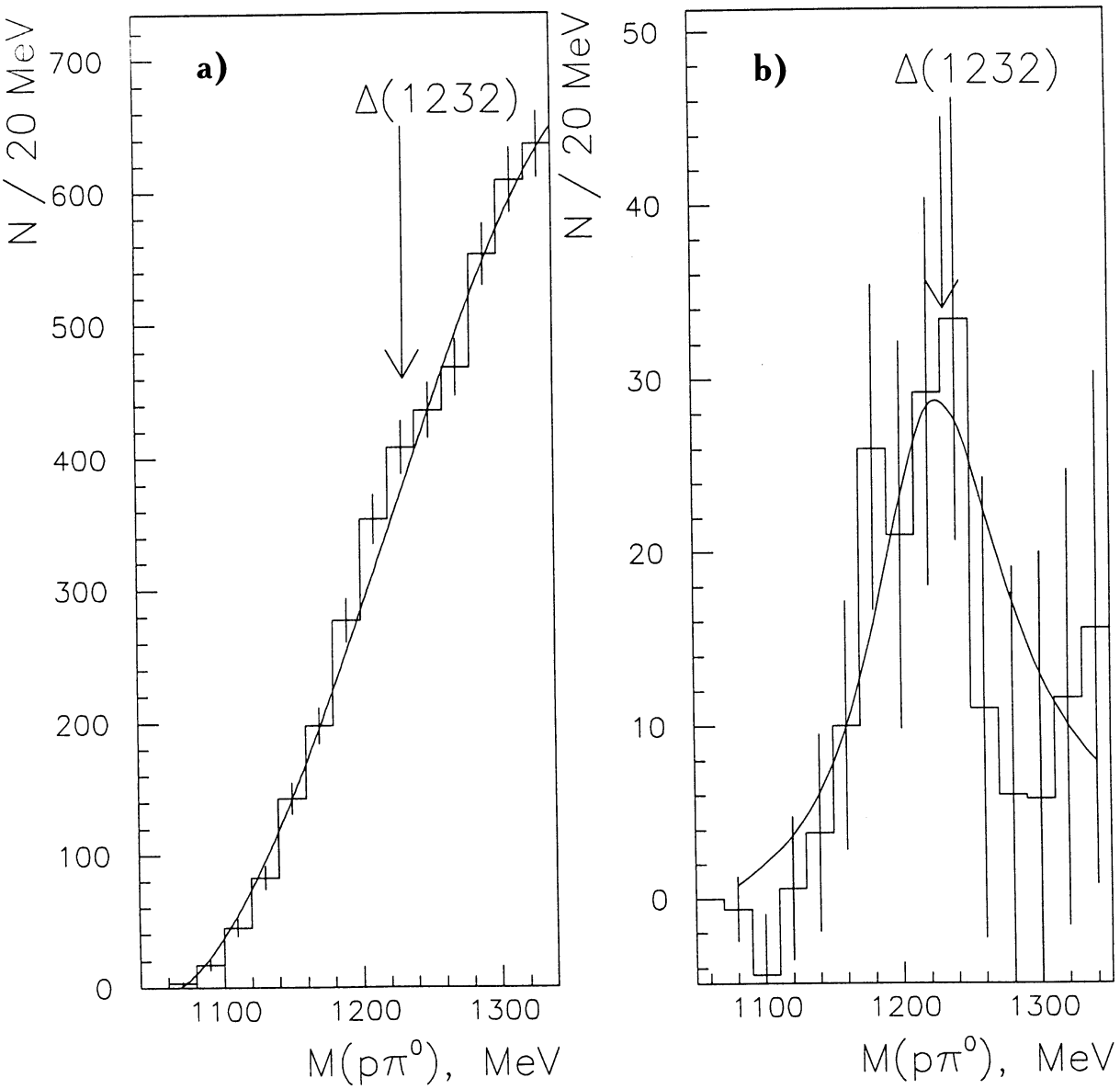

Figure 10: The Coulomb production of isobar $\Delta(1232)^+$ in the coherent reaction $p+C \to \Delta(1232)^+ + C$; $\Delta(1232)^+ \to p\pi^0 \to p\gamma[\gamma \to e^+e^-]$ in the SPHINX experiment. Because of the trigger requirment we used the decay $\pi^0 \to \gamma[\gamma \to e^+e^-]$ with e^+e^--conversion of one of the photons in the setup target for π^0-detection. a) The effective mass spectrum $M(p\pi^0)$ for the diffractive reaction $p+N \to [p\pi^0]+N$ (all P_T^2). There is no evidence for $\Delta(1232)^+$ in this mass spectrum because Δ isobar (with isospin $I = 3/2$) cannot be produced in the diffractive dissosiation of the proton. b) $M(p\pi^0)$ mass spectrum for the coherent reaction $p + C \to [p\pi^0] + C$ in the Coulomb region ($P_T^2 < 0.01$ GeV^2) after the subtruction of diffractive $p\pi^0$ background. A clear peak with parameters $M = (1232 \pm 10)$ MeV and $\Gamma = (119 \pm 20)$ MeV which corresponds to the Coulomb production of $\Delta(1232)^+$ isobar is seen in this mass spectrum.

References

[1] Primakoff H., Phys. Rev., 1951, vol. 81, p.119.

[2] Pomeranchuk I.Ya., Shmushkevich I.M., Nucl. Phys., B, 1961, vol. 23, p. 452.

[3] Bityukov S.I. et al., Yad.Fiz., 1988, vol. 47, p. 1258.

[4] Weidenauer, p. et al., Z.Phys. C, 1990, vol. 47, p.353.

[5] Alde D. et al., Phys.Lett.B, 1994, vol. 340, p. 122.

[6] Binon F. et al., Yad. Fiz., 1981, vol. 203, p. 327.

[7] Bityukov, S.I. et al., Phys.Lett.B, 1988, vol. 203, p. 327.

[8] Landsberg L.G. Fiz. Elem. Chastits At.Yadra, 1990, vol. 21, p. 1054.

[9] Djhelyadin R.I. et al., Phys.Lett.B, 1980, vol. 94, p. 548.

[10] Victorov V.A. et al., Yad.Fiz., 1980, vol. 32, p. 1005.

[11] Landsberg L.G., Phys., Rep., 1985, vol. 128, p. 301.

[12] Zielinski M., Acta Phys. Polonica B, 1987, vol. 18, p. 455.

[13] O'Donnel P.J., Rev. Mod. Phys. 1981, vol. 53, p. 673.

[14] H.Kolanoski, Springer Tracts Mod.Phys., 1984, vol. 105.

[15] Halpern A. et al., Phys.Rev., 1966, vol. 152, p. 1295.

[16] Dreitlein J., Primakoff H., Phys.Rev., 1962, vol. 125, p. 591.

[17] Berlad G. et al., Annals of Phys., 1973, vol. 75, p. 461.

[18] Fäldt G. et al., Nucl.Phys.B., 1972, vol. 41, p. 125; vol. 43, p. 591.

[19] Jansen T. et al., Phys.Rev.D, 1983, vol. 27, p. 26.

[20] Huston J. et al., Phys.Rev.D, 1986, vol. 33, p. 3199.

[21] Cihangir S. et al., Phys.Lett.B, 1982, vol. 117, p. 119.

[22] Zeilinski M. et al., Phys.Rev.Lett., 1984, vol. 52, p. 1195.

[23] Collick B. et al., Phys.Rev.Lett., 1984, vol. 53, p. 2374.

[24] Berg D. et al., Phys.Lett.B, 1981, vol. 98, p. 119.

[25] Carismith D. et al., Phys.Rev.Lett., 1986, vol. 56, p. 18.

[26] Carismith D. et al., Phys.Rev.D, 1986, vol. 36, p. 3199.

[27] Capraro L. et al., Nucl.Phys.B, 1987, vol.288, p. 659.

[28] Antipov Yu.M. et al., Phys.Lett.B, vol. 121, p. 445.

[29] Antipov Yu.M. et al., Phys.Rev.D, vol. 121, p. 445.

[30] Dydak F., et al., Nucl.Phys.B, 1977, vol. 118, p.1; Delvin T. et al., Phys.Rev.D, vol. 34, p. 1626.

[31] Peterson P.C. et al. Phys.Rev.Lett., 1986, vol. 57, p. 949.

[32] Kubarowsky V.P., Report on ICHEP-98, Vancouver, July, 1998.

[33] Landsberg L.G., Yad.Fiz. (in press)

[34] Edelstein R. et al., Fermilab Proposal E781, 1987 (revised 1993); Russ J.S., Nisl.Phys, 1995, vol. 585A, p. 39c.

[35] Smith V.J., Hadron Spectroscopy ("Hadron-97"), Seventh Intern. Conf., Upton, NY, August 1997, (ed, Chung, S-U., Willutzki, H.J.) p. 627.

[36] Zielinski M. et al., Z. Phys.C, 1983, vol. 16, p. 197.

[37] Babcock J., Rosner J. L., Phys.Rev., 1976, vol. 14D, p. 1286.

[38] Ishida S. et al., Phys.Rev, 1989, vol 40D, p. 1497.

[39] Landsberg L.G., Yad.Fiz., 1996, vol. 59, p. 2161.

[40] Landsberg L.G., Molchanov V.V., Preprint IHEP 97-42, Protvino, 1997.

[41] Hogaasen H., Sorba P., Nucl.Phys.B, 1978, vol. 145, p. 119.

[42] Chan Hoang-Mo, Tsou S.T., Nucl.Phys.B, 1977, vol. 118, p. 413.

[43] Hirose T. et al., Nuov. Cim.A, 1979, vol. 50A,

[44] Landsberg L.G., Yad.FiZ. 1994, vol. 57, p. 47; UFN, 1994, vol. 164, p. 1129.

[45] Zielinski M. et al., Z.Phys.C, 1986, vol. 31, p. 545; vol. 34, p. 255.

[46] Landsberg L.G., Yad.Fiz., 1990, vol. 52, p. 192; Landsberg L.G., Nucl.Phys.,B (proc.Suppl.), 1991, vol.21, p. 179.

[47] Vavilov D.V. et al. Yad.Fiz., 1999, vol.62 (in press).

[48] Shumacher R., Preprint CMU MEG-96-007, Pittsburg, 1996.

[49] Caso C. et al. (PDG), The Europ. Phys.Journ., 1998, vol. 3, N1-4, p.1.

[50] Vavilov D.V. et al., Yad.Fiz. 1995, vol. 58, p. 1426.

[51] Vavilov D.V. et al., Yad.Fiz. 1994, vol. 57, p. 241.

[52] Bezzubov V.A. et al., Yad.Fiz., 1996, vol. 59, p. 2199.

[53] Golovkin S.V. et al., Z.Phys., 1995, vol. 68C, p. 585.

[54] Landsberg L.G., Yad.Fiz., 1997, vol. 60, p. 1541.

[55] Landsberg L.G., Phys.Rep. (in press).